Numerical study of temperature oscillation in loop heat pipe

著者	Takuya Adachi, Koji Fujita, Hiroki Nagai
journal or publication title	Applied Thermal Engineering
volume	163
page range	114281
year	2019-12-25
URL	http://hdl.handle.net/10097/00133522

doi: 10.1016/j.applthermaleng.2019.114281

Numerical study of temperature oscillation in loop heat pipe

Takuya Adachi[a*], Koji Fujita[b] and Hiroki Nagai[b]

[a]*Department of Aerospace Engineering, Tohoku University, 2-1-1, Katahira, Aoba-ward, Sendai 980-8579, Japan.*

[b]*Institute of Fluids Science, Tohoku University, 2-1-1, Katahira, Aoba-ward, Sendai 980-8577, Japan.*

HIGHLIGHTS

- Once a two-phase flow is generated in the liquid line, temperature oscillation occurs.
- A low reservoir temperature leads to a two-phase flow in the liquid line.
- When the condensation length oscillates highly, temperature amplitude becomes high.
- Low sink temperature can prevent temperature oscillation.

ABSTRACT

Loop heat pipes are high-efficient heat transfer devices. Many spacecraft have loop heat pipes to control the temperature of equipment precisely. Temperature oscillation, however, sometimes occurs in the loop heat pipe when the external conditions change. Temperature oscillation may impede the temperature-controlling ability of loop heat pipes. Nevertheless, the cause of temperature oscillation has not been understood yet. To understand the internal flow during temperature oscillation, we developed a transient model that can reproduce the fluid condition in the transport lines. In this study, the reservoir temperature, the liquid line temperature, and the condensation length were focused. Investigating the relation between each parameter, we found that the cause of temperature oscillation is the inflow of two-phase flow into the liquid line, which is caused by decreasing the reservoir temperature. In addition, as the amplitude of the condensation length becomes high, temperature amplitude also becomes high. When the sink temperature is low, the condensation length can barely oscillate, and thus, temperature oscillation is less likely to occur.

Keywords: Loop heat pipe, Temperature oscillation, Transient model, Condensation length

---

A	:	Cross-sectional area (m^2)
C	:	Heat capacity (J/K) or parameter in Lockhart‐Martinelli model
c_p	:	Specific heat (J/(kg·K))
d	:	Diameter (m)
dt	:	Time step (s)
G	:	Thermal conductance (W/K)
Gr	:	Grashof number
h	:	Enthalpy (J/(kg·K))
h_{lv}	:	Latent heat (J/kg)
h_{nc}	:	Natural convection heat-transfer coefficient (W/(m^2·K))
h_{tc}	:	Heat-transfer coefficient (W/(m^2·K))
k	:	Thermal conductivity (W/(m·K))
L	:	Length (m)
m	:	Mass (kg)
$\dot{m}$	:	Mass flow rate (kg/s)

*Corresponding author.

E-mail address: adachi.takuya@space.ifs.tohoku.ac.jp

Nu : Nusselt number
P : Pressure (Pa)
Pr : Prandtl number
$\dot{Q}$: Amount of heat transferred between the fluid in the pipe and the ambient or the sink (W)
$\dot{Q}_{in}$: Heat load (W)
Re : Reynolds number
Su : Suratman number
T : Absolute temperature (K)
u : flow velocity (m/s)
UA/L : Thermal conductance per unit length (W/(m·K))
V : Volume (m^3)
x : Vapor quality
X : Lockhart-Martinelli parameter
z : Coordinate in axial direction
ε : Porosity
μ : Viscosity (Pa·s)
ρ : Density (kg/s)
σ : Surface tension (N/m)
ϕ : Two-phase multiplier

Subscript
air : Air
amb : Ambient
bulk : Wick material
cc : Reservoir
cond : Condenser
eff : Effective
evap : Evaporator or evaporation
f : Fluid
hb : Heater block
i : Node number
in : Inner
int : Vapor-liquid interface
l : Liquid
ll,out : Liquid line outlet
out : Outer
sat : Saturation
sink : Sink
tp : Two-phase flow
v : Vapor
vg : Vapor groove
wall : Wall

1. Introduction

Loop heat pipes (LHPs) are highly-efficient and reliable heat transfer devices [1–3]. Many spacecrafts mount LHPs for thermal control. Fig. 1 shows the schematic of an LHP. The LHP has working fluid and consists of an evaporator, vapor line, condenser, liquid line, and reservoir. The heat applied to the evaporator is absorbed by evaporation, and the generated vapor condenses in the condenser. The LHP can transport a large amount of heat. The evaporator and condenser are connected with simple pipes. The capillary force of a primary wick in the evaporator circulates the working fluid. The LHP can precisely control the temperature of equipment with a small amount of electric power. As the LHP has many advantages, there have been several studies on the ground application of the LHP [4–7].

One of the problems in the LHP, however, is temperature oscillation. When the heat load applied to the evaporator or the temperature of the sink attached to the condenser changes, the temperature of the LHP sometimes oscillates. This may impede the temperature-control capabilities of an LHP and may cause equipment failure when the allowable temperature range of the equipment becomes narrow.

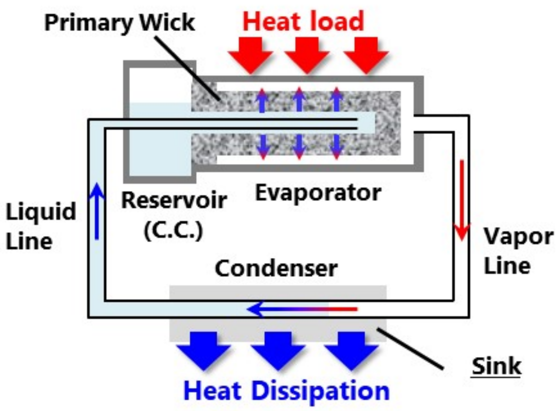

Fig. 1 Schematic of a loop heat pipe

Various investigations on temperature oscillation have been conducted. Ku et al. observed two types of temperature oscillation in the experiments: high-amplitude/low-frequency oscillation [8] and low-amplitude/high-frequency oscillation [9]. According to the previous research [8], when the thermal mass attached to the evaporator is high, the heat load applied to the evaporator is kept to a minimum, and the sink temperature is lower than the ambient temperature, high-amplitude/low-frequency oscillation occurs. They also found that the amplitude of temperature becomes high as the condensation length (the length required for vapor to completely condense) oscillates highly [8].

On the other hand, the cause of the low-amplitude/high-frequency oscillation has not been understood yet. The proposed experiment mainly focuses on the low-amplitude/high-frequency oscillation. Ku et al. [9] predicted that the temperature oscillation would occur if the condensation length is either longer or shorter than the condenser length. Chen et al. [10] also led to the same conclusion as Ku [9] and elucidated the influence of the LHP orientation on the temperature oscillation. Vershinin et al. [11] investigated the favorable conditions for the temperature oscillation. They concluded that the shortage of the working fluid in the LHP and the shortage of the liquid in the reservoir caused the temperature oscillation. However, the cause of the temperature oscillation has been only deduced based on the experimental results.

Numerical simulation is useful to understand the cause of the temperature oscillation. Some researchers developed transient models of LHPs [12–19]. There are only a few transient models related to temperature oscillation. Launay et al. [15] developed a transient model for the temperature oscillation that yielded good accordance with the experimental results. Hoang et al. [16] proposed the stability theory for the LHP based on the analytical model. The stability criteria proposed in their research indicated that the higher the degree of the subcooling in the liquid line, the higher the possibility of temperature oscillation.

However, the relation between the internal flow and temperature oscillation is still unclear. The previous researches have not elucidated the reason why temperature oscillation occurs when the condensation length becomes longer than the condenser length or when the degree of the subcooling in the liquid line is high. In this study, we developed an analytical model to understand the internal flow during temperature oscillation. The model can calculate the vapor quality in the transport lines and investigate the fluid condition.

2. Analytical model

The LHP is modeled, especially focusing on the internal flow of the vapor line, the condenser, and the liquid line. The analytical model is divided into two parts: the vapor line, the condenser and the liquid line; the evaporator and the reservoir. The fluid is assumed to be incompressible and viscous.

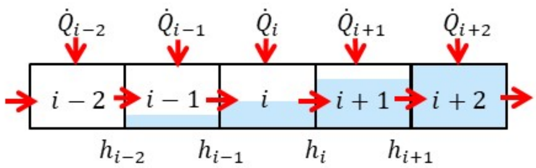

Fig. 2 Discretization of vapor line, condenser, and liquid line

2.1 Vapor line, condenser, and liquid line

The vapor line, condenser, and liquid line are discretized into small-volume nodes (Fig. 2). i expresses the node number and starts from the vapor line inlet. The energy-conservation equation at node i is expressed as

$$\left[\rho V \frac{dh}{dt}\right]_i = \dot{m}(h_{i-1} - h_i) + \dot{Q}_i + u_i A(P_{i-1} - P_{i+1}) + \frac{kA}{dz}(T_{i-1} - T_i) + \frac{kA}{dz}(T_{i+1} - T_i). \quad (1)$$

$\dot{Q}_i$ in the vapor line and the liquid line is calculated by

$$\dot{Q}_i = G_{f\_amb}(T_{amb} - T_i). \quad (2)$$

G_{f_amb} is given as follows.

$$\frac{1}{G_{f\_amb}} = \frac{G_{f\_wall} + G_{wall}}{G_{f\_wall} \cdot G_{wall}} + \frac{1}{G_{wall\_amb}}. \quad (3)$$

G_{wall_amb} is calculated using the natural convection heat transfer coefficient. The Nusselt number to determine the natural convection heat transfer coefficient is calculated by

$$Nu = 0.74\left(Gr \cdot P_{r_{air}}\right)^{1/15}. \quad (4)$$

$\dot{Q}_i$ in the condenser is expressed as

$$\dot{Q}_i = (UA/L)_{cond} \cdot dz \cdot (T_{sink} - T_i). \quad (5)$$

$(UA/L)_{cond}$ is difficult to calculate theoretically and therefore assumed to be 4 W/(m·K) based on Ref. [20].

The vapor quality in each node is calculated as follows to investigate fluid condition.

$$x_i = \frac{h_i - h_{l,sat}}{h_{v,sat} - h_{l,sat}}. \quad (6)$$

h_i is calculated from Eq. (1). The vapor quality basically takes a value from 0 to 1 and shows the vapor mass flow rate. If the vapor quality is higher than 1, it means that the fluid in that node is superheated vapor. If the vapor quality is lower than 0, the fluid in that node is subcooled liquid.

When the fluid is superheated vapor or subcooled liquid, the Nusselt number for a laminar and a turbulent flow is expressed as

$$Nu = \begin{cases} 3.66 & \text{(laminar)} \\ 0.023 \cdot Re^{0.8} \cdot P_r^{\,0.3} & \text{(turbulant).} \end{cases} \quad (7)$$

The heat transfer coefficient of a two-phase flow is expressed as follows [22].

$$h_{tc_i} = h_{tc,l} \times \left\{(1 - x_i)^{0.8} + \frac{3.8x^{0.76}(1 - x_i)^{0.04}}{(P_i/P_{cr})^{0.38}}\right\}. \quad (8)$$

The pressure in each node is calculated by

$$P_i = P_{i-1} - \Delta P_i \qquad \text{for } i \neq 1, \quad (9)$$

$$P_i = P_{vg} - \Delta P_i \qquad \text{for } i = 1. \quad (10)$$

The pressure drop is calculated based on the Darcy-Weisbach equation if the fluid is a single-phase flow.

The pressure drop of a two-phase flow is calculated based on the Lockhart-Martinelli method [23]. The pressure drop of a two-phase flow is calculated by

$$\left(\frac{dP}{dz}\right)_{tp} = {\phi_l}^2 \left(\frac{dP}{dz}\right)_l. \tag{11}$$

${\phi_l}^2$ is calculated by

$${\phi_l}^2 = 1 + \frac{C}{X} + \frac{1}{X^2}, \tag{12}$$

where X is expressed as

$$X^2 = \frac{(dP/dz)_l}{(dP/dz)_v}. \tag{13}$$

To calculate C in Eq. (12), Kim's model [21] is used. The value of C is expressed as shown in Table 1. Re_{lo} and Su_{vo} in Table 1 are given as follows.

$$Re_{lo} = \frac{4\dot{m}}{\pi \mu_l d_{in}}, \tag{14}$$

$$Su_{vo} = \frac{\rho_v \sigma d_{in}}{{\mu_v}^2}. \tag{15}$$

Table 1 Kim's method for calculating C [21]

Liquid	**Vapor**	**Parameter C**
Turbulent	Turbulent	$0.39{Re_{lo}}^{0.03}{Su_{vo}}^{0.10}\left(\frac{\rho_l}{\rho_v}\right)^{0.35}$
Laminar	Turbulent	$0.0015{Re_{lo}}^{0.59}{Su_{vo}}^{0.19}\left(\frac{\rho_l}{\rho_v}\right)^{0.36}$
Turbulent	Laminar	$8.7 \times 10^{-4}{Re_{lo}}^{0.17}{Su_{vo}}^{0.50}\left(\frac{\rho_l}{\rho_v}\right)^{0.14}$
Laminar	Laminar	$3.5 \times 10^{-5}{Re_{lo}}^{0.44}{Su_{vo}}^{0.50}\left(\frac{\rho_l}{\rho_v}\right)^{0.48}$

2.2 Evaporator and reservoir

The evaporator model is divided into the heater block, the evaporator wall, the vapor groove, and the primary wick. The energy conservation equation for each part is solved to calculate temperature. The energy conservation equation for the heater block is expressed as

$$C_{hb}\frac{dT_{hb}}{dt} = \dot{Q}_{in} - \dot{Q}_{hb\_evap} - \dot{Q}_{hb\_amb}. \tag{16}$$

The energy conservation for the evaporator wall is expressed as

$$C_{evap,wall}\frac{dT_{evap,wall}}{dt} = \dot{Q}_{hb\_evap} - \dot{Q}_{evap\_vg} - \dot{Q}_{evap\_wick} - \dot{Q}_{evap\_cc}. \tag{17}$$

The energy conservation equation for the vapor in the vapor groove is expressed as

$$\rho_v c_{p_v} V_{vg}\frac{dT_{vg}}{dt} = \dot{Q}_{evap\_vg} - \dot{m}c_{p_v}(T_{vg} - T_{int}). \tag{18}$$

The vapor-liquid interface is saturated. The interface temperature is the saturation temperature of the pressure applied in the vapor groove. The pressure in the vapor groove is the sum of the reservoir pressure and the capillary force of the primary wick. The capillary force is equal to the total pressure drop in the LHP. Therefore, the pressure of the vapor groove is expressed as

$$P_{vg} = P_{cc} + \Delta P_{total}, \tag{19}$$

where ΔP_{total} is the total pressure drop in the LHP.

The primary wick is discretized in the radial direction as shown in Fig. 3. The amount of heat conducted from node *i* to node *i – 1* is expressed as

$$\dot{Q}_{i\_i-1} = \frac{2\pi L_{wick} k_{eff}}{\ln(d_i/d_{i-1})}(T_{wick,i} - T_{wick,i-1}), \tag{20}$$

where k_{eff} is calculated as

$$k_{eff} = (1-\varepsilon)k_{bulk} + \varepsilon k_l. \tag{21}$$

When *i* is equal to 1, the amount of heat conducted to the reservoir is expressed as

$$\dot{Q}_{wick\_in} = \frac{2\pi L_{wick} k_{eff}}{\ln(d_1/d_{wick,in})}(T_{wick,1} - T_{cc}). \tag{22}$$

The energy conservation equation at the innermost node of the primary wick is expressed as

$$(\rho c_p)_{eff} V_1 \frac{dT_{wick,1}}{dt} = \dot{Q}_{2\_1} - \dot{Q}_{wick\_in} - \dot{m}c_{p_l}(T_{wick,1} - T_{cc}), \tag{23}$$

where $(\rho c_p)_{eff}$ is calculated by

$$(\rho c_p)_{eff} = (1-\varepsilon)(\rho c_p)_{bulk} + \varepsilon(\rho c_p)_l. \tag{24}$$

The energy conservation equation at the innermost node of the primary wick is expressed as

$$(\rho c_p)_{eff} V_n \frac{dT_{wick,n}}{dt} = \dot{Q}_{evap_{wick}} - \dot{Q}_{n_n-1} - \dot{m}c_{p_l}(T_{int} - T_{wick,n-1}) - \dot{m}_{evap}h_{lv} \tag{25}$$

$\dot{m}_{evap}$ is calculated by the following equation.

$$\dot{m}_{evap}h_{lv} = h_{evap}A(T_{evap,wall} - T_{int}). \tag{26}$$

The evaporation heat transfer coefficient h_{evap} varies with temperature. The heat transfer coefficient, however, is assumed to be constant. The energy conservations at other nodes are expressed as

$$(\rho c_p)_{eff} V_i \frac{dT_{wick,i}}{dt} = \dot{Q}_{i+1_i} - \dot{Q}_{i_i-1} - \dot{m} c_{p_l}\left(T_{wick,i} - T_{wick,i-1}\right). \tag{27}$$

The energy conservation in the reservoir is expressed as

$$m_{cc} c_{p_{cc}} \frac{dT_{cc}}{dt} = \dot{Q}_{wick\_in} + \dot{Q}_{evap\_cc} - \dot{m} c_p\left(T_{cc} - T_{ll,out}\right) - \frac{kA}{dz}\left(T_{cc} - T_{ll,out}\right) - \dot{Q}_{cc\_amb}. \tag{28}$$

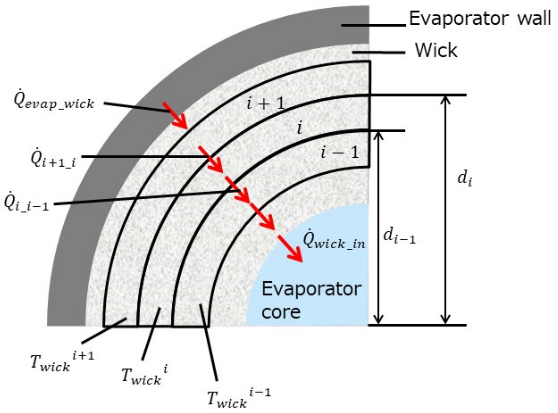

Fig. 3 Discretization of the primary wick

Table 2 LHP geometry

Evaporator		**Vapor line**	
Length	100.0 mm	Length	800.0 mm
Outer/Inner diameter	19.0/16.0 mm	Outer/Inner diameter	4.85/2.85 mm
Primary wick		**Liquid line**	
Length	67.0 mm	Length	1100 mm
Pore radius	7.0 µm	Outer/Inner diameter	4.85/2.85 mm
Permeability	10^{-13}m^2	**Condenser**	
Porosity	50%	Outer/Inner diameter	6.35/4.35 mm
Outer/Inner diameter	16.0/7.0 mm	Length	1200 mm
Groove height/width	2.12/3.22 mm	**Reservoir**	
Groove length	60 mm	Outer/Inner diameter	45.0/43.0 mm
The number of grooves	7	Length	25.0 mm

2.3 Calculation Conditions

Table 2 shows the LHP geometry used in this study. The geometry is determined based on the experiments of Riehl et al. [24]. The primary wick is made of an ultra-high molecular weight polyethylene, and other parts are made of stainless steel. The working fluid is acetone, and the ambient temperature is 19°C.

3. Results and discussion

Fig. 4 shows temperatures at the evaporator wall (Evap. Wall), condenser inlet (Cond. Inlet), liquid line inlet (L.L. Inlet), and reservoir (Resv.) where the heat load is 20 W and the sink temperature is 10 °C. In this case, temperatures converge. In the experiment of Riehl et al. [24], the convergence temperature of the evaporator was 320 K when the heat load is 20 W, and the temperature of the cooling bath is – 5 °C. The temperature difference between the calculation and the experiment of Riehl at al. [24] is caused by the difference of the evaporation heat transfer coefficient and that of the ability to cool the condenser. The heat transfer coefficient must vary with temperature, but is assumed to be constant in this model. Although the cooling bath temperature is different between the calculation and the experiment of Riehl et al. [24], the temperature of condenser outlet is same at 284 K. However, this LHP model can reproduce the basic operation of the LHP and is qualitatively correct. Fig. 5 shows temperature when the heat load is 40 W. In this case, temperature oscillation occurs, and we will discuss the internal flow based on the calculation results.

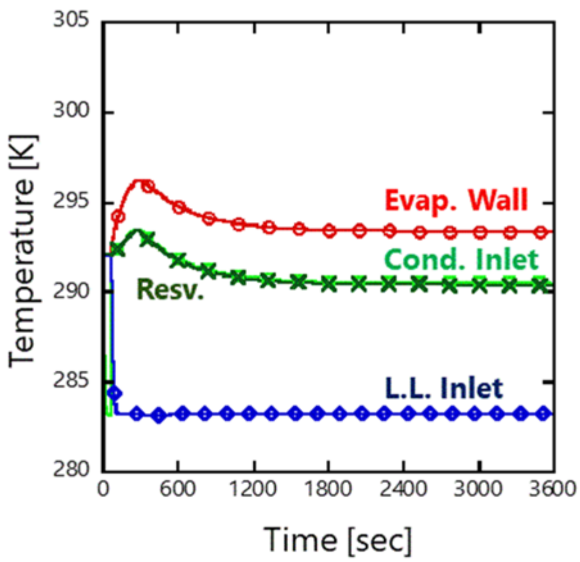

Fig. 4 Temperature history
(Heat load is 20 W, sink temperature is 10 °C.)

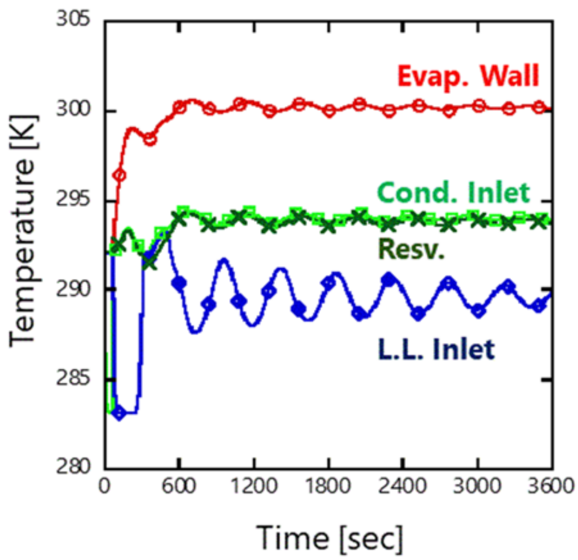

Fig. 5 Temperature history
(Heat load is 40 W, sink temperature is 10 °C.)

3.1 Internal flow at the start of temperature oscillation

The internal flow at the start of the temperature oscillation is investigated. As shown in Fig. 5, the liquid line inlet temperature rapidly rises before the temperature oscillation starts. To explain that reason, Fig. 6 shows the reservoir temperature, the liquid line inlet temperature, and the vapor quality at the liquid line inlet. When the liquid line temperature rises rapidly, the vapor quality becomes greater than 0 (the line (a) in Fig. 6). It means that a two-phase flow penetrates the liquid line. This causes the rapid rise in the liquid line temperature. After the two-phase flow is generated in the liquid line, the two-phase flow returns to the subcooled liquid (the line (b) in Fig. 6). Now, the liquid line temperature starts to drop, and then the temperature oscillation occurs. In Ref. [9,10], the authors predicted that the cause of temperature oscillation is the vapor penetrating to the liquid line. This result is in accordance with these previous researches. However, after the two-phase flow in the liquid line return to the subcooled liquid (after the line (b) in Fig. 6), it does not get regenerated in the liquid line.

The generation of the two-phase flow is caused by the low reservoir temperature. The reservoir temperature is almost the same as the saturation temperature in the LHP because the proportion of reservoir volume to the whole is large. When the reservoir temperature is low, the vapor becomes difficult to condense, and the two-phase flow is generated in the liquid line. Hoang et al. [16] suggested that the high degree of a liquid subcooling in the liquid line causes temperature oscillation. The calculation result is also in accordance with Hoang's suggestion because the liquid's high degree of the subcooling will lower the reservoir temperature. Therefore, when a subcooled liquid from the liquid line decreases the reservoir temperature, and when a two-phase flow is generated in the liquid line, the temperature oscillation will start.

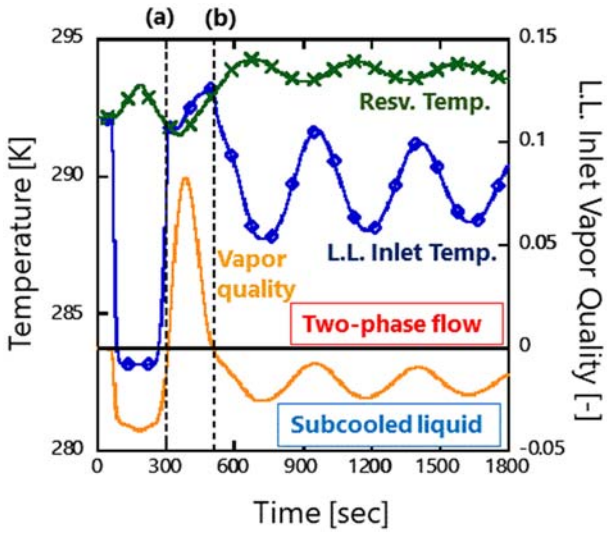

Fig. 6 The relationship between the fluid condition in the liquid line and temperature in the liquid line and the reservoir

3.2 Internal flow during stable temperature oscillation

To understand the internal flow during temperature oscillation, we focus on the condensation length, which is the length from the condenser inlet to the position where the vapor is completely condensed. Fig. 7 shows the condensation length during temperature oscillation (Heat load is 40 W, sink temperature is 10 °C), and a two-phase flow is generated in the liquid line only once. However, when the sink temperature becomes 15 °C, the two-phase flow repeatedly penetrates in the liquid line (See Fig. 10).

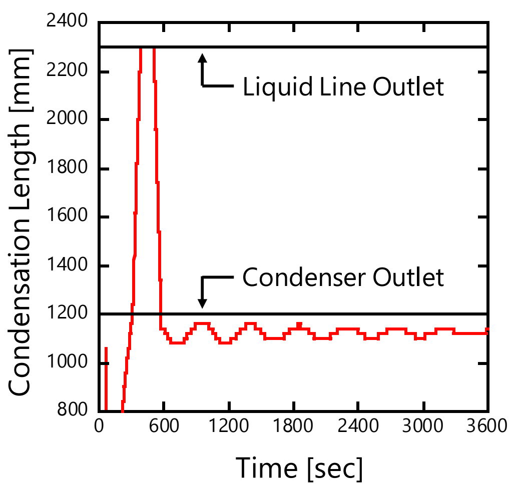

Fig. 7 The condensation length
(Heat load is 40 W, sink temperature is 10 °C.)

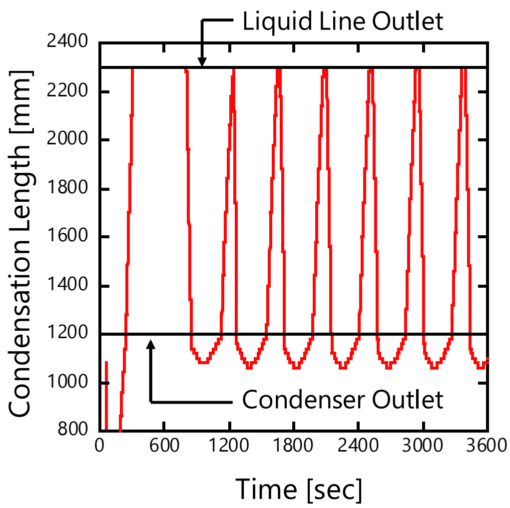

Fig. 8 The condensation length
(Heat load is 40 W, sink temperature is 15 °C.)

Fig. 9 shows the temperature amplitude in the liquid line inlet against the amplitude of the condensation length when the condensation length oscillates in the condenser like Fig. 7. The temperature amplitude at the liquid line inlet is proportional to the amplitude of the condensation length. Fig. 10 shows the temperature amplitude in the liquid line inlet against the minimum condensation length in the case where the condensation length oscillates over the condenser length like Fig. 8. The temperature at the liquid line inlet is affected only by the fluctuation of the condensation length in the condenser, which can be expressed as the difference between the condenser length and the local minimum condensation length during steady oscillation. The short minimum condensation length indicates the high amplitude of the condensation length in the condenser. Therefore, Figs. 9 and 10 show that the high-amplitude of the condensation length causes the high-temperature amplitude. The high-amplitude of the condensation length indicates that the subcooled region in the condenser fluctuates significantly. The fluid temperature is decreased only in the subcooled region because the heat is released for phase-change in the two-phase region. It means that the long subcooled region reduces the liquid line inlet temperature. Therefore, the fluctuation of the condenser length is important for temperature amplitude. According to Ref. [8], the same phenomenon was observed when the high-amplitude/low-frequency oscillation occurred. Our calculation indicates that the relationship between the temperature amplitude and the condensation length is the same for the high-amplitude/low-frequency oscillation and low-amplitude/high-frequency oscillation.

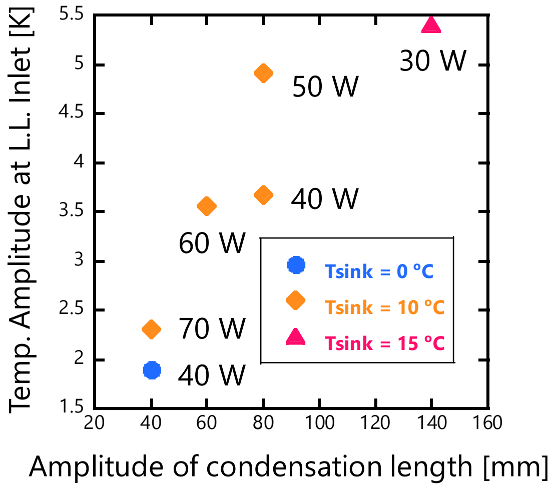

Fig. 9 The relationship between the temperature amplitude and the amplitude of the condensation length (The condensation length oscillates in the condenser.)

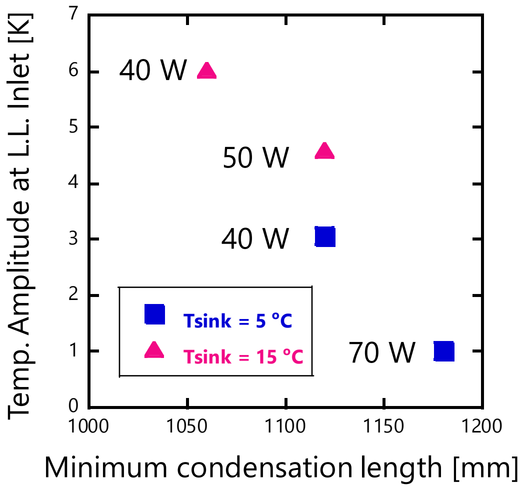

Fig. 10 The relationship between the temperature amplitude and the minimum condensation length (The condensation length oscillates over the condenser length.)

3.3 Influence of the heat load and the sink temperature

Fig. 11 shows the reservoir temperature for each heat load. The sink temperature is 10 °C. The temperatures start to oscillate when the heat load is larger than 40 W. When the heat load is high, the degree of subcooling in the liquid line becomes low, and the reservoir temperature does not drop much. Therefore, the temperature oscillation is less likely to occur at a high heat load.

Fig. 12 shows the reservoir temperature for each sink temperature. The heat load is 40 W. When the sink temperature is lower than 0 °C, temperatures converge smoothly. The reason why the low sink temperature can prevent the temperature from oscillating is related to the condensation length. As mentioned above, the liquid's high degree of the subcooling is necessary to cause the temperature oscillation, and low sink temperature will lead to a high degree of the subcooling. However, when the sink temperature is low, a large amount of heat is released in the narrow region. At this time, a condensation length is very hard to be changed and does not change enough to cause temperature oscillation. Therefore, even if the two-phase flow is generated in the liquid line due to the low reservoir temperature, temperature oscillation can be prevented by the low sink temperature.

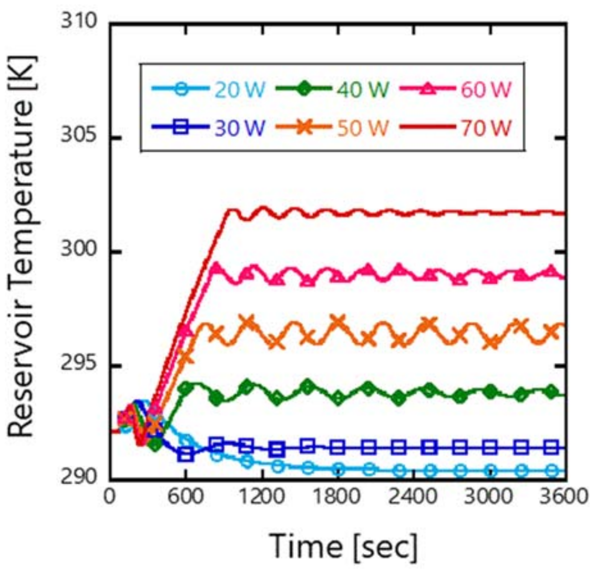

Fig. 11 Reservoir temperature at different heat loads

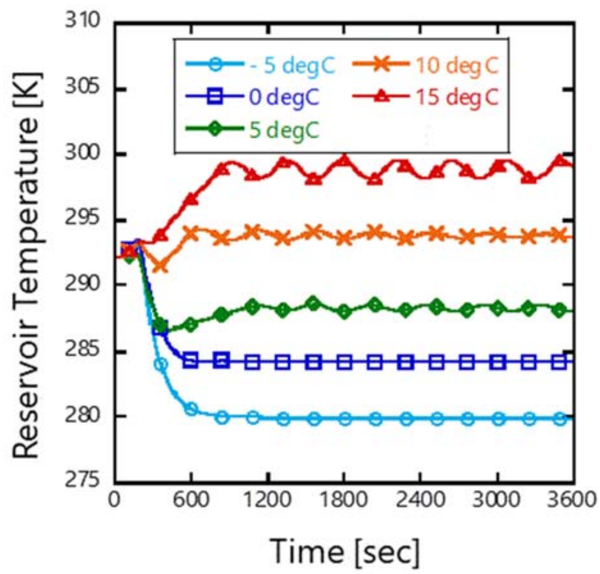

Fig. 12 Reservoir temperature at different sink temperature

4. Conclusions

We investigated the internal flow of an LHP during the temperature oscillation by using the transient model. The calculation results show that the cause of temperature oscillation is the penetration of the two-phase flow into the liquid line, which is caused by the low reservoir temperature. After the penetration of the two-phase flow, when the reservoir temperature rises enough, the subcooled liquid flows in the liquid line. Even if the penetration of the two-phase flow in the liquid line occurs only once, temperature oscillation occurs. In addition, we found that when the condensation length starts to oscillate highly, the temperature amplitude becomes high. The condensation length must continue to fluctuate to keep oscillating temperature.

6. References

[1] J. Ku, Operating Characteristics of Loop Heat Pipes, in: Proc. 29th Int. Conf. Environ. Syst., Denver, Colorado, 1999. doi:10.4271/1999-01-2007.

[2] Y.F. Maydanik, Loop heat pipes, Appl. Therm. Eng. 25 (2005) 635–657. doi:10.1016/j.applthermaleng.2004.07.010.

[3] S. Launay, V. Sartre, J. Bonjour, Parametric analysis of loop heat pipe operation: a literature review, Int. J. Therm. Sci. 46 (2007) 621–636. doi:10.1016/j.ijthermalsci.2006.11.007.

[4] V.G. Pastukhov, Y.F. Maidanik, C. V. Vershinin, M.A. Korukov, Miniature loop heat pipes for electronics cooling, Appl. Therm. Eng. 23 (2003) 1125–1135. doi:10.1016/S1359-4311(03)00046-2.

[5] J. Li, F. Lin, D. Wang, W. Tian, A loop-heat-pipe heat sink with parallel condensers for high-power integrated LED chips, Appl. Therm. Eng. 56 (2013) 18–26. doi:10.1016/j.applthermaleng.2013.03.016.

[6] N. Putra, B. Ariantara, R.A. Pamungkas, Experimental investigation on performance of lithium-ion battery thermal management system using flat plate loop heat pipe for electric vehicle application, Appl. Therm. Eng. 99 (2016) 784–789. doi:10.1016/j.applthermaleng.2016.01.123.

[7] J. Esarte, J.M. Blanco, A. Bernardini, J.T. San-José, Optimizing the design of a two-phase cooling system loop heat pipe: Wick manufacturing with the 3D selective laser melting printing technique and prototype testing, Appl. Therm. Eng. 111 (2017) 407–419. doi:10.1016/j.applthermaleng.2016.09.123.

[8] J. Ku, J. Rodriguez, Low Frequency High Amplitude Temperature Oscillations in Loop Heat Pipe Operation, in: Proc. 33rd Int. Conf. Environ. Syst., Vancouver, Canada, 2003. doi:10.1360/zd-2013-43-6-1064.

[9] J. Ku, L. Ottenstein, M. Kobel, P. Rogers, T. Kaya, Temperature Oscillation in Loop Heat Pipe Operation, in: AIP Conf. Proc., 2001: pp. 255–262.

[10] Y. Chen, M. Groll, R. Mertz, Y.F. Maydanik, S. V. Vershinin, Steady-state and transient performance of a miniature loop heat pipe, Int. J. Therm. Sci. 45 (2006) 1084–1090. doi:10.1016/j.ijthermalsci.2006.02.003.

[11] S. V. Vershinin, Y.F. Maydanik, Investigation of pulsations of the operating temperature in a miniature loop heat pipe, Int. J. Heat Mass Transf. 50 (2007) 5232–5240. doi:10.1016/j.ijheatmasstransfer.2007.06.024.

[12] T. Hoang, J. Ku, Transient Modeling of Loop Heat Pipes, in: 1st Int. Energy Convers. Eng. Conf., Portsmouth, Virginia, 2003. doi:10.2514/6.2003-6082.

[13] T. Kaya, J. Goldak, Numerical analysis of heat and mass transfer in the capillary structure of a loop heat pipe, Int. J. Heat Mass Transf. 49 (2006) 3211–3220. doi:10.1016/j.ijheatmasstransfer.2006.01.028.

[14] M. Nishikawara, H. Nagano, T. Kaya, Transient Thermo-Fluid Modeling of Loop Heat Pipes and Experimental Validation, J. Thermophys. Heat Transf. 27 (2013) 641–647. doi:10.2514/1.T3888.

[15] S. Launay, V. Platel, S. Dutour, J.-L. Joly, Transient Modeling of Loop Heat Pipes for the Oscillating Behavior Study, J. Thermophys. Heat Transf. 21 (2007) 487–495. doi:10.2514/1.26854.

[16] T.T. Hoang, R.W. Baldauff, J.R. Maxwell, Stability Theory for Loop Heat Pipe Design , Analysis and Operation, in: Proc. 45th Int. Conf. Environ. Syst., Bellevue, Washington, 2015.

[17] T.T. Hoang, R.W. Baldauff, C.E. Tiu, Verification of Loop Heat Pipe Stability Theory − Part I Low-Frequency/High-Amplitude Oscillations, in: Proc. 45th Int. Conf. Environ. Syst. Int. Conf. Environ. Syst., Bellevue, Washington, 2015.

[18] V. V. Vlassov, R.R. Riehl, Mathematical model of a loop heat pipe with cylindrical evaporator and integrated reservoir, Appl. Therm. Eng. 28 (2008) 942–954. doi:10.1016/j.applthermaleng.2007.07.016.

[19] L. Bai, G. Lin, D. Wen, Modeling and analysis of startup of a loop heat pipe, Appl. Therm. Eng. 30 (2010) 2778–2787. doi:10.1016/j.applthermaleng.2010.08.004.

[20] T. Kaya, J. Ku, A Parametric Study of Performance Characteristics of Loop Heat Pipes, in: Proc. 29th Int. Conf. Environ. Syst., Denver, Colorado, 1999.

[21] S.M. Kim, I. Mudawar, Universal approach to predicting two-phase frictional pressure drop for adiabatic and condensing mini/micro-channel flows, Int. J. Heat Mass Transf. 55 (2012) 3246–3261. doi:10.1016/j.ijheatmasstransfer.2012.02.047.

[22] M.M. Shah, A general correlation for heat transfer during film condensation inside pipes, Int. J. Heat Mass Transf. 22 (1979) 547–556. doi:10.1016/0017-9310(79)90058-9.

[23] R.W. Lockhart, R.C. Martinelli, Proposed Correlation of Data for Isothermal Two-Phase, Two-Component Flow in Pipes, Chem. Eng. Prog. 45 (1949) 39–48.

[24] R.R. Riehl, T. Dutra, Development of an experimental loop heat pipe for application in future space missions, Appl. Therm. Eng. 25 (2005) 101–112. doi:10.1016/j.applthermaleng.2004.05.010.